# Elastic imaging with OBS receiver-side multiples

*Yuting Duan* and Paul Sava, Center for Wave Phenomena, Colorado School of Mines*


## SUMMARY

Receiver-side water-layer multiples acquired with ocean bottom seismometers (OBS) can be used for elastic imaging of the subsurface. Multiples can be separated from the data acquired at the OBS receivers by up/-down decomposition. The down-going field corresponds to multiples which characterize just P waves since the last propagation leg is in water. OBS elastic reverse-time migration exploits mode conversion from P to S as the injected multiples travel through the ocean bottom interface. As for acoustic migration, multiples are injected into the model from virtual receivers located on a surface, symmetric relative to the ocean surface, thus increasing the imaging aperture. The elastic images for different combinations of P and S modes suffer from cross-talk between non-physical wave modes. However, this cross-talk is characterized by moveout in shot-domain common-image gathers, and therefore it can be filtered out after imaging.


## INTRODUCTION

Seismic acquisition with ocean bottom seismometers is a rapidly developing technology meant to address significant challenges in marine acquisition. In particular, OBS acquisition is used to acquire high-fold data in areas with dense infrastructure. A common acquisition setup uses ocean bottom nodes which enable acquisition of four-component (4C) data consisting of pressure and particle velocity using a hydrophone and a geophone, respectively. Nodes are usually sparsely distributed on the ocean bottom (OB) due to their high cost and deployment difficulty. This sparse acquisition is compensated by a dense network of sources at the ocean surface (OS). This setup enables acquisition of wide-azimuth data which is invaluable in imaging complex geologic structures (Berg et al., 2010). Furthermore, the four-component acquisition facilitates separation of acquired data into up-going and down-going waves, as well as into P or S wave-modes (Schalkwijk, 2001). This separation enables elastic imaging, which potentially provides access to lithologic information.

Although usually strong, the receiver-side first-order water-layer multiples are often treated as noise and removed from the acquired data. Imaging is usually performed using the primaries separated at the OB. However, as discussed by various authors (Godfrey et al., 1998), multiples contain additional information compared with primaries and provide increased illumination of the subsurface. Furthermore, the receiver-side multiples are just P modes since they propagate in water, although they may originate as S reflections in the subsurface.

Imaging with multiples is usually carried out by assuming that the receivers are located on a virtual horizon above the OS and representing the mirror of the OB (Dash et al., 2009; Ronen et al., 2005; Wong et al., 2011). This acquisition geometry provides a much wider illumination of the subsurface, especially in deep water.

OBS imaging with receiver-side multiples is usually performed under the acoustic assumption. Both primaries (up-going) and multiples (down-going) are treated as purely acoustic modes in imaging and velocity analysis (Lu et al., 2009; Wong et al., 2011). In this paper, we generalize this idea to elastic imaging with OBS data, in order to generate images of the subsurface corresponding to illumination by both P and S modes. For this purpose, we make use of the fact that the P modes propagating into the water layer convert to S modes while crossing the OB. Then, we can use elastic RTM with an imaging condition based on wave-modes separated using Helmholtz decomposition (Yan and Sava, 2007) to produce images of all possible combinations of P and S modes extracted from the source and receiver wavefields.

Our methodology relies heavily on mode conversions at the OB. Some of the P-to-S conversions correspond to physical events, i.e. they represent S-to-P conversions of waves propagating from the subsurface. However, other P-to-S conversions are not physical, but merely an artifact of the elastic extrapolation during migration. Such "fake" conversions generate artifacts into the image and may overlap with real reflectors in the subsurface. However, we find that such fake events are not consistent in image gathers produced with multiple seismic experiments, but show moveout that can be used to differentiate them from real reflections.

## THEORY

Our procedure for elastic imaging with OBS data consists of several steps, as outlined next.

### Up/down separation

Data acquired by ocean-bottom seismometers consist of pressure $P$ and particle velocity $\mathbf{V}$ and correspond to waves propagating both upward (mainly primaries) and downward (multiples). Assuming that the ocean bottom is horizontal, we can separate the P-modes propagating upward ($U$) or downward ($D$) using the expressions (Grion et al., 2007)

$$U = \frac{1}{2}P + \alpha\, V_z \,, \tag{1}$$

$$D = \frac{1}{2}P - \alpha\, V_z \,, \tag{2}$$

where $V_z$ represents the vertical component of the particle velocity vector, and $\alpha$ is a scale factor. If the OB is not horizontal, then we can simply rotate the particle velocity vector such that $V_z$ corresponds to the normal to the water/solid interface.

The scale factor $\alpha$ in equations 1 and 2 can be defined in many different ways (Barr and Sanders, 1989; Amundsen, 1993; Richwalski, 2000; Schalkwijk, 2001) as a function of the wave incidence angle and the material properties (density and P or S velocities). Here, we do not emphasize this separation in any more detail, but simply assume that we can use one of the existing procedures to obtain the up-going and down-going modes, thus having access to the primaries and multiple reflections, respectively. However, we note that both up-going and down-going modes potentially contain other multiples (higher order surface-related multiples or internal multiples), although we assume that these are lower amplitude and do not contribute much to imaging. We also note that the down-going mode contains both P energy propagating from the subsurface through the ocean bottom, as well as S energy that converts to P as it crosses the ocean bottom, Figures 1(a)-1(d).

**Elastic wavefield reconstruction**

Using the separated up-going and down-going wave-modes, we can proceed with elastic reverse-time migration, which includes numeric reconstruction of the source and receiver wavefields. On the source side, we simulate elastic wavefields using a pressure source located at the known position near the surface. On the receiver side, we simulate elastic wavefields using the separated up-going and down-going wavefields as sources in the water column. The injected P-modes propagate through the ocean bottom as P, but also convert to S as they cross the liquid/-solid interface. Some of these conversions correspond to real waves that have propagated from reflectors in the subsurface, but other conversions lead to fake modes that do not represent a physical reality. Such fake modes produced artifacts in the migrated images.

**Elastic imaging condition**

The reconstructed source and receiver elastic wavefields can be separated into P and S modes prior to imaging (Yan and Sava, 2007). In isotropic media, this separation can be done using the Helmholtz decomposition theorem (Aki and Richards, 2002) based on the displacement vector $\mathbf{u}(\mathbf{x}, t)$:

$$P = \nabla \cdot \mathbf{u} \,, \qquad (3)$$

$$\mathbf{S} = \nabla \times \mathbf{u} \,. \qquad (4)$$

The vector shear wave mode $\mathbf{S}$ describes two degenerate waves which are indistinguishable in isotropic media. Here, we avoid this complication by discussing the case of a 2D earth, in which case the S mode can be considered a vector with only one component, and thus can be treated as a scalar. Therefore, we can use the imaging condition formulated by Yan and Sava (2007) to combine different wave modes for the source and receiver wavefields, and obtain 4 independent images:

$$R^{ij}(x, z, t) = \sum_t {W_s}^i(x, z, t)\, {W_r}^j(x, z, t) \;. \qquad (5)$$

Here, $R$ represents the reflectivity, $W_s$ and $W_r$ are source and receiver wavefields, respectively, and $i$ and $j$ indicate the wave-mode used in imaging, e.g. P or S. The cartoons in Figures 1(a)-1(d) show the propagation paths for different combinations of incident and reflected P and S modes. In all cases, the multiple energy propagating in the water is represented only by P waves, although in some cases this P energy comes from conversion of S energy at the ocean bottom (Figure 1(b) and Figure 1(d)) or from conversion from P to S at the ocean bottom, followed by conversion from S to P at a reflector, e.g. Figure 1(c).

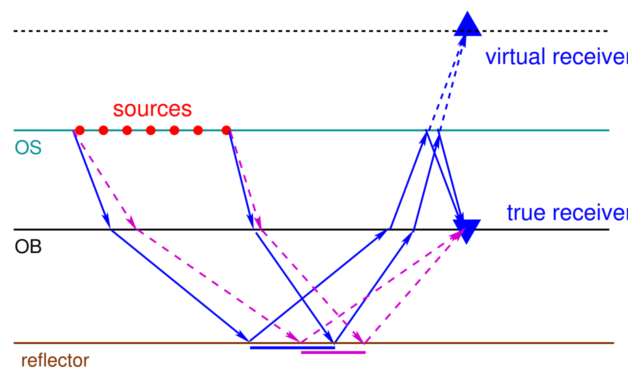


Figure 2: Different illumination patterns in the subsurface for primary (dashed lines) and water layer multiples (solid lines).

**Mirror imaging**

Primary and multiple images are characterized by different effective aperture, thus leading to different illumination patterns in the subsurface. This can be conceptually explained by considering that the receivers for the multiple energy are located on a virtual horizon represented by the mirror of the ocean bottom relative to the surface, as shown in Figure 2, (Pica et al., 2006). Since the receivers are now located at a larger distance from the sources, the effective aperture is proportionally larger, in particular in the case of deep water. In the case of sparse sources and dense receivers, migration with primary reflected waves is characterized by wider angle illumination, compared to mirror imaging. However, OBS acquisition is characterized by dense sources on the water surface and sparse receivers on the ocean floor; therefore multiple imaging provides wider aperture than primary imaging, Figure 2.

**Artifact removal**

As indicated earlier, the receiver wavefields reconstructed in the subsurface contain fake wave modes due to unphysical conversions at the ocean floor. Real and fake wave modes correlate with one-another, thus generating artificial reflectors similar to the interference between

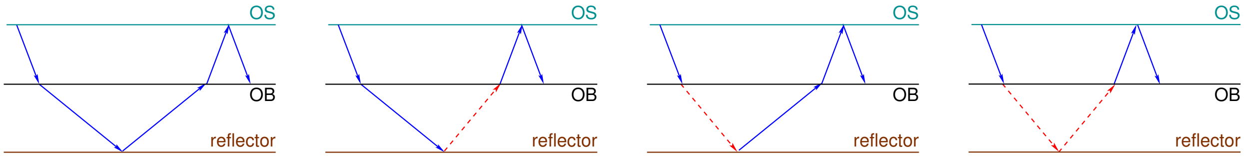


(a) (b) (c) (d)

Figure 1: Schematic representation of the receiver-side first-order surface-related multiples. The solid lines represent P-waves and the dashed lines represent S-waves. From left to right, the panels correspond to PP, PS, SP and SS reflections.

primaries and multiples in conventional PP imaging. These artifacts, however, are generally inconsistent from shot to shot; therefore they appear as events with moveout in various kinds of gathers where they can be filtered by various techniques, e.g. Radon transforms (Sava and Guitton, 2005) or plane-wave destructors (Fomel, 2002). This assumes that the model used for imaging is accurate, in which case the true reflections are flat as a function of shot, even if their polarity changes, as is the case for the PS and SP images. This separation is not trivial, since some artifacts could be significantly stronger than the real reflection, e.g. for the weak SS reflections which can be overwhelmed by artifacts of other kinds, e.g. PS, SP, or even PP. We do not elaborate more on this subject in this paper.

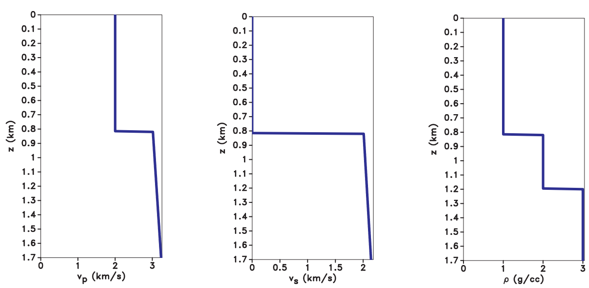


(a) (b) (c)

Figure 3: (a) P-wave velocity (b) S-wave velocity and (c) density profiles in the 2D synthetic model.

## EXAMPLES

We illustrate our method with a 2D model consisting of one horizontal reflector under the OB, Figures 3(a)-3(c). The receivers are located on the OB at $z = 0.8$ km, although in the migrated images we extend the imaging space to $z = -0.8$ km in order to capture the mirror receivers. Figures 4(a)-4(d) and 5(a)-5(d) show imaging with primaries injected into the model at the true receivers, and imaging with water-related multiples injected into the model at the virtual receivers, respectively. The figure show, from top to bottom, PP, PS, SP and SS images, respectively. All images correspond to one pressure source located on the OS at $z = 0$ km. However, the side panels in all figures display one common-image gather (CIG) at $x = 3.0$ km for dense shots distributed all over the OS.

In all cases, we observe the reflector at its true depth, $z = 1.2$ km, as well as numerous cross-talk artifacts due to interference of fake P or S modes, as well as multiple reflections of various kinds. In the PP image, many artifacts occur in the water layer, and can be simply eliminated by muting, but some cross-talk artifacts occur in the elastic zone under the OB, i.e. $z > 0.8$ km, and interfere with the true reflector. However, as seen in the CIGs shown next to each image, only the true reflection is characterized by a horizontal event as a function of shot, and can thus be preserved in the image through attenuation of all other events with moveout. As indicated earlier, this separation is not trivial because some of the artifacts are stronger than the image, but it can nevertheless be done using conventional methodology like Radon transforms or plane-wave destruction.

Finally, we note that primary and multiple images have different illumination patterns, and their combination expands the illumination areas of the subsurface. This conclusion is true for all images combining P and S modes, regardless of the changing polarity on opposite sides of the shot.

## CONCLUSIONS

We demonstrate the potential of receiver-side first-order water layer multiples for elastic imaging. Our method uses P-mode injection, followed by conversion to S-modes at the OB. Images for different combinations of P and S modes are obtained after mode separation from extrapolated elastic wavefields using Helmholtz decomposition. Multiples are imaged using the conventional approach with receivers simulated on a mirror of the OB relative to the OS. This procedure widens the imaging aperture and improves illumination. We show that elastic images are contaminated by cross-talk artifacts caused by fake wave-modes or multiples. However, common-image gathers adequately separate the influence of the true reflectors from the cross-talk artifacts, thus offering the potential for accurate elastic imaging of the subsurface using OBS multiple energy.

## ACKNOWLEDGMENTS

We thank sponsor companies of the Consortium Project on Seismic Inversion Methods for Complex Structures, whose support make this research possible. The reproducible numeric examples in this paper use the Madagascar open-source software package freely available from http://www.ahay.org.


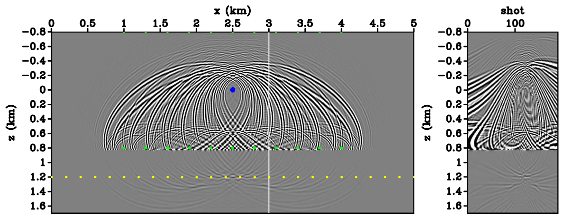


(a)

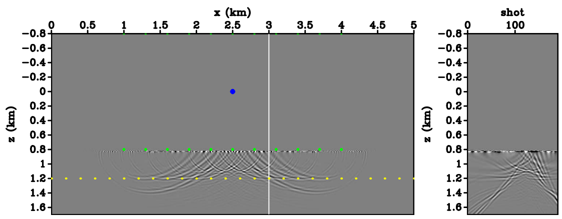


(b)

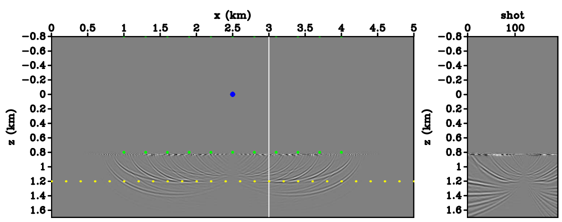


(c)

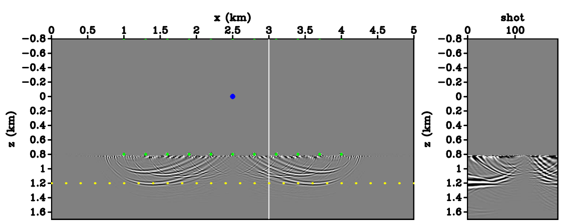


(d)

Figure 4: Migrated images of OBS **primary** reflections: (a) PP, (b) PS, (c) SP and (d) SS reflectivity.

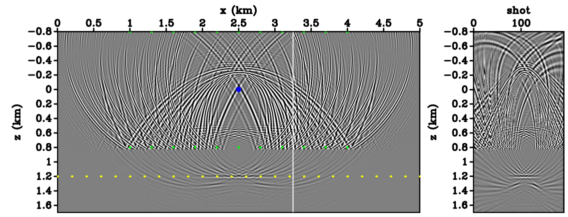


(a)

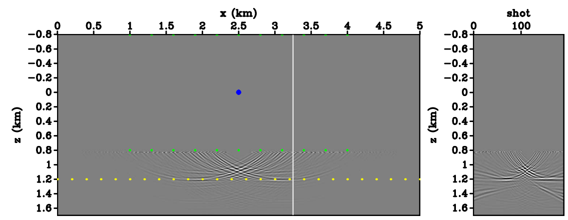


(b)

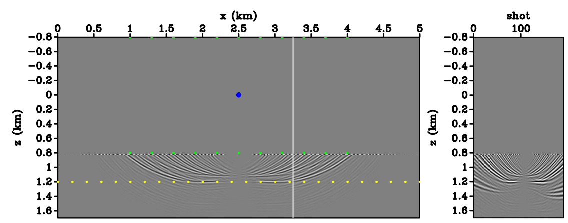


(c)

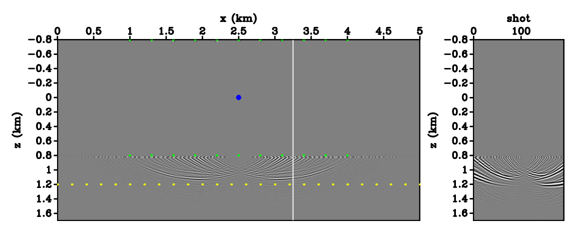


(d)

Figure 5: Migrated images of OBS **multiple** reflections: (a) PP, (b) PS, (c) SP and (d) SS reflectivity.

## REFERENCES


Aki, K., and P. Richards, 2002, Quantitative seismology (second edition): University Science Books.

Amundsen, L., 1993, Wavenumber-based filtering of marine point-source data: Geophysics, **58**, 1335–1348.

Barr, F. J., and J. L. Sanders, 1989, Attenuation of water-column reservations using pressure and velocity detectors in a water-bottom cable: 59th Annual International Meeting, SEG, Expanded Abstracts, 653–656.

Berg, E., C. Vuillermoz, G. Ekmann, and G. Woje, 2010, Origin and advances of the planted 4C seismic node technology: 80th Annual International Meeting, SEG, Expanded Abstracts, 3728–3733.

Dash, R., G. Spence, R. Hyndman, S. Grion, Y. Wang, and S. Ronen, 2009, Wide-area imaging from OBS multiples: Geophysics, **74**, Q41–Q47.

Fomel, S., 2002, Applications of planewave destruction filters: Geophysics, **67**, 1946–1960.

Godfrey, R. J., P. Armstrong, B. Cooper, and E. Thorogood, 1998, Imaging the foinaven ghost: 68th Annual International Meeting, SEG, Expanded Abstracts, 1333–1335.

Grion, S., R. Exley, M. Manin, X. Miao, A. Pica, Y. Wang, P. Granger, and S. Ronen, 2007, Mirror imaging of OBS data: First Break, **25**, 37–42.

Lu, R., P. Traynin, and J. E. Anderson, 2009, Comparison of elastic and acoustic reverse-time migration on the synthetic elastic marmousi-II OBC dataset: 79th Annual International Meeting, SEG, Expanded Abstracts, 2799–2803.

Pica, A., M. Manin, P. Y. Granger, D. Martin, E. Suaudeau, B. David, G. Poulain, and P. Herrmann, 2006, 3D SRME on OBS data using waveform multiple modeling: 76th Annual International Meeting, SEG, Expanded Abstracts, 2659–2663.

Richwalski, S. M., 2000, Multi-component wavefield separation with application to land seismic data: PhD thesis, Utrecht University, Netherlands.

Ronen, S., L. Comeaux, and X. Miao, 2005, Imaging downgoing waves from ocean bottom stations: 75th Annual International Meeting, SEG, Expanded Abstracts, 963–966.

Sava, P., and A. Guitton, 2005, Multiple attenuation in the image space: Geophysics, **70**, V10–V20.

Schalkwijk, K. M., 2001, Decomposition of multicomponent ocean-bottom data into p- and s-waves: PhD thesis, Delft University of Technology.

Wong, M., S. Ronen, and B. Biondi, 2011, Least-squares reverse time migration/inversion for ocean bottom data: a case study: 81st Annual International Meeting, SEG, Expanded Abstracts, 2369–2373.

Yan, J., and P. Sava, 2007, Elastic wavefield imaging with scalar and vector potentials: 77th Annual International Meeting, SEG, Expanded Abstracts, 2150–2154.